Received September 8, 2020, accepted September 19, 2020, date of publication September 22, 2020,
date of current version October 6, 2020.

Digital Object Identifier 10.1109/ACCESS.2020.3025860

Photovoltaic Power Forecasting With a Hybrid Deep Learning Approach

GANGQIANG LI[1,2], SEN XIE[2,3], BOZHONG WANG[4], JIANTAO XIN[1], YUNFENG LI[1], AND SHENGNAN DU[5]

[1]College of Electronics and Information Engineering, Shenzhen University, Shenzhen 518060, China
[2]College of Mechatronics and Control Engineering, Shenzhen University, Shenzhen 518060, China
[3]College of Physics and Optoelectronic Engineering, Shenzhen University, Shenzhen 518060, China
[4]State Grid Hunan Electric Power Corporation Maintenance Company, Changsha 410082, China
[5]College of Electrical and Information Engineering, Hunan University, Changsha 410082, China

Corresponding author: Sen Xie (senxie@szu.edu.cn)

This work was supported in part by the National Natural Science Foundation of China under Grant 61903257, in part by the National Natural Science Foundation of Guangdong Province under Grant 2018A030310523, and in part by the Special Innovation Project in Higher Education of Guangdong Province under Grant 2018KTSCX351.

ABSTRACT Solar energy is the key to clean energy, which can generate large amounts of electricity for the future smart grid. Unfortunately, the randomness and intermittency of solar energy resources bring difficulties to the stable operation and management of the power systems. To reduce the negative impact of photovoltaic (PV) plants accessing on the power systems, it is great significant to predict PV power accurately. In light of this, we propose a hybrid deep learning approach based on convolutional neural network (CNN) and long-short term memory recurrent neural network (LSTM) for the PV output power forecasting. The CNN model is leveraged to discover the nonlinear features and invariant structures exhibited in the previous output power data, thereby facilitating the prediction of PV power. The LSTM is used to model the temporal changes in the latest PV data, and predict the PV power of next time step. Then, the prediction results in the two models are comprehensively considered to obtain the expected output power. The proposed approach is extensively evaluated on real PV data in Limberg, Belgium, and numerical results demonstrate that the proposed approach can provide good prediction performance in PV systems.

INDEX TERMS Solar energy, deep learning, photovoltaic (PV) power forecasting, power systems.

I. INTRODUCTION

Distributed energy resources (DERs), such as wind energy and solar energy, have developed rapidly across the world and played an important role in the power systems [1], [2]. Especially, solar energy, as a renewable energy source, is complete free, accessible and scalable [3]. Meanwhile, solar energy is the key to clean energy future, which can generate large amounts of electricity via the solar panels without burning fossil fuels. Many energy legislations and incentives have been established worldwide to improve the penetration rate of solar power in future smart grid [4]. However, the randomness and intermittency of solar power bring difficulties to the stable operation and management of the power grid [5]. These uncertainties will also reduce the real-time control performance and economic benefits, which is not conducive to the large-scale expansion of photovoltaic (PV) power plants. The prediction methods for forecasting the PV power accurately have become important tool to solve PV planning and modeling problems, which can alleviate the negative impacts on the entire power system and improve the stability of the system [6]. With the development of advanced electricity meters in current power grid, richer source data can be used to build more sophisticated forecasting models to achieve more accurate PV power forecasting [7].

Generally, more accurate forecasting of solar power plays a crucial role in smart grids. In the grid-connected PV systems, the efficiency of the forecasting schedule depends on the accuracy of the forecasting, and the reliable prediction results of PV load are utilized to calculate some multi-objective tasks [8]. In [9], the accurate prediction of PV power generation has positive effects on the control strategies of PV-battery energy storage systems, such as improving the self-consumption of PV systems and reducing power flows

The associate editor coordinating the review of this manuscript and approving it for publication was Bin Zhou.

to the grid. In [10], a deterministic forecasting module is presented in a smart energy management system to optimize the operation of the microgrid. In addition, the PV forecasting technology is widely used in hybrid integrated energy systems [11]–[13], real-time electric vehicle charging scheduling and management [14], [15], multi-objective optimization tasks [16], [17], robust planning electric vehicle charging facilities [18], and smart home energy management [19].

So far, the PV power forecasting approaches are divided into three categories: 1) statistical methods; 2) physical methods; 3) artificial intelligent learning methods [20]. Statistical methods try to establish the functional mapping relationship between historical data and output power, such instance time series method [21], regression analysis method [22], gray theory [23]. The statistical models often rely on historical data and need to exclude morbid data points that are not conducive to these models. Unlike the statistical methods, physical methods do not require the support of a large amount of historical data, but it studies the characteristics of PV power generation equipment and establishes the corresponding mathematical model for power forecasting [24]. The meteorological and geological parameters used for physical mathematical models are usually measured by numerical weather prediction (NWP) or ground measurement devices. However, physical methods require appropriate and frequently calibrated service facilities [25], [26]. Artificial intelligent learning methods benefit from the rapid growth of computing power and exploit artificial intelligence algorithm to learn a mapping relationship between input and output, mainly focusing on nonlinear mapping models [27]–[29]. Artificial intelligence methods have been widely used in various domains, ranging from abnormal detection [30], power grids [31], [32], energy consumption [33], pattern recognition [34]–[36], and have become an excellent tool for PV power generation prediction [37], [38].

With PV power generation prediction technology as the core, artificial intelligence methods extract the nonlinear features of historical data related to PV system effectively, thus leading more competitive prediction performance than statistical and physical methods [39]. In addition, artificial intelligence methods can predict PV output power directly from readily accessible data without complex calculations and other high costs. For example, in [40], a high-precision deep neural network model was proposed to forecast the output power of the PV system. Moreover, a BPNN prediction model considering seasonal weather classification was established to forecast the PV power outputs [41]. In [42], the authors proposed a simplified approach to predict the 24-h ahead of PV power in an experimental roof-top PV system by using radial basis function neural network (RBFNN). In [43], three distinct artificial neural network (ANN) models were developed to forecast the PV production accurately. In [4], wavelet decomposition and convolutional neural network (CNN) were used to predict PV power for 2-hours ahead. The authors in [44] utilized long-short term memory recurrent neural network (LSTM) to forecast the power of PV systems accurately.

However, the above-mentioned methods do not take into account the prior information of adjacent days, and thus discard the critical weather changes of the PV data. A natural extension in this context is that more accurate prediction performance is explored if the forecasting model considers the prior information of adjacent days. Therefore, we originally propose a hybrid method based on CNN and LSTM to forecast the PV output power. Herein, the CNN is used to discover the nonlinear features and invariant structures of the prior power data that are exhibited simultaneously on different dates. The LSTM based prediction model takes the previous PV power data on the same date as input and predicts the PV power of next time. After that, the predicted PV power is reconstructed according to prediction results of CNN and LSTM. The main contributions of this article can be summarized as follows:

(1) We analysis the PV output power of adjacent days and show the prior power data simultaneously on different dates, which are conducive to improve prediction performance of PV systems.

(2) We propose a hybrid deep learning framework based on CNN and LSTM. The proposed method considers the prior data of adjacent days when constructing the prediction model.

(3) We take the real PV data in Limberg, Belgium, and numerical results demonstrate the effectiveness of the proposed method.

The paper is organized as follows. In Section II, we analysis the historical data of PV output power. In Section III, a hybrid architecture based on CNN and LSTM for predicting PV output power is proposed. Numerical results and analysis are given in Section IV. We conclude this work in Section V.

II. PHOTOVOLTAIC POWER DATA ANALYSIS

A. THE PV POWER DATA

We consider a historical PV power dataset over one year, the daily data covers the time period from 5:00 to 19:00, with a 15-min resolution. Let D be the number of days in a period of PV data, and M be the number of power points in a day. $p_d^m \in \mathbf{R}$ for $m \in [1, \ldots, M]$ and $d \in [1, \ldots, D]$ be the m th power point of the dth day. By putting $\{p_d^m\}_{d,m}$ together, we can get an output power matrix $\tilde{P} \in \mathbf{R}^{D\times M}$, ie.,

$$\tilde{\boldsymbol{P}} = \begin{bmatrix} p_1^1 & \cdots & p_1^M \\ \cdots & \cdots & \cdots \\ p_D^1 & \cdots & p_D^M \end{bmatrix} \tag{1}$$

Denote $\boldsymbol{p}_d = [p_d^1, \ldots, p_d^M]^T \in \mathbf{R}^M$ as the output power of the dth day. $\boldsymbol{p}_m = [p_1^m, \ldots, p_D^m]^T \in \mathbf{R}^D$ is the mth column vector of $\tilde{\boldsymbol{P}}$, which includes the mth output power point on different days. As shown in Fig. 1, the PV output power in Flanders from July 1 to July 10 is given. Fig. 2 shows the PV output power in July from 10:00 o'clock to 14:00 o'clock.

In Fig. 1, it can be seen that the PV power sequence changes in the adjacent days have a certain continuity. For instance,

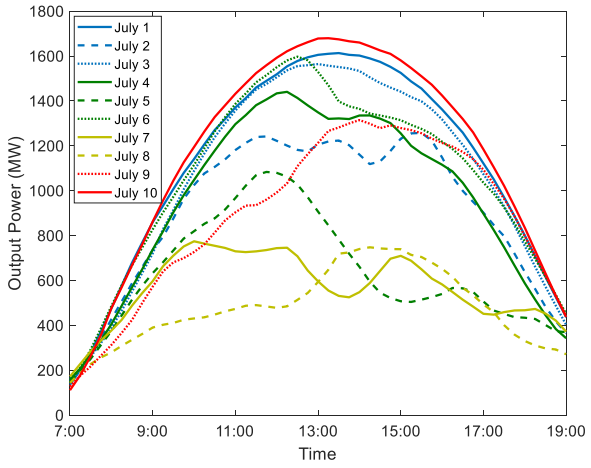

FIGURE 1. The output PV power curves of adjacent days in Limberg.

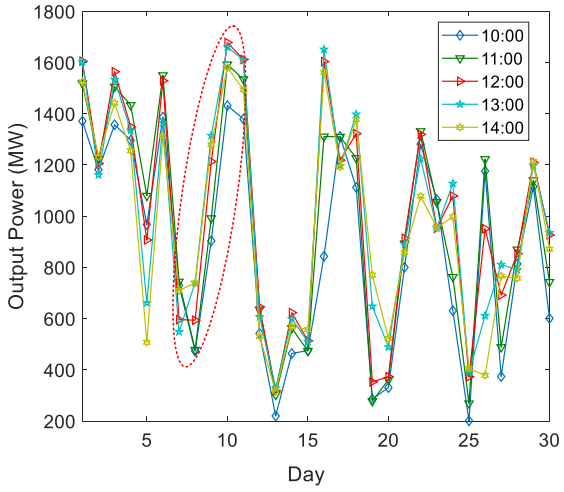

FIGURE 2. The output PV power at the same time on different dates.

for the seventh and eighth sequences, the output power in these two days is similar, and it can be inferred that the weather in these two days is also similar. For the eighth, ninth and tenth sequences, the output power of these days has increased significantly over time, and maybe the weather condition on the tenth day is more suitable for the production of PV plants. That is to say the output power sequences of adjacent days can reflect the changing trend of weather conditions. With a high chance, the day after a sunny day may also be a sunny day, and the day after a rainy day may become another rainy day instead of a sunny day [45]. Inevitably, the output power of the second day may be quite different from that of the previous day due to the chaotic nature of the weather conditions, as seen in the fifth, sixth and seventh sequences. However, the output power sequences of adjacent days can provide more weather information for future PV power forecasting.

Moreover, the output power point at the same time on different days is plotted in Fig. 2. Obviously, the output power points at the same has a strong uncertainty on different dates, and the sequence is not stable. This makes sense that the weather conditions are the essential determinant of the solar energy. From the red dotted lines, the output power increases approximately linearly with the increase of the date. As can be seen that the PV power point at the same time of previous days can be used to predict the PV power of the next day for short-term prediction. In addition, an artificial intelligence method is leveraged to learn a mapping relationship between input and output.

B. CORRELATION BETWEEN THE ADJACENT DAYS

To explore the correlation between the output power of different dates, we consider a historical output power dataset $\tilde{\boldsymbol{P}}$ over one year, $D = 360$. The data resolution is 15 minutes per day, covering a period from 5:00 o'clock to 19:00 o'clock, $M = 60$. The output power for the ith day is $\boldsymbol{p}_i = [p_i^1, \ldots, p_i^M]^T, \forall i \in [1, \ldots, D]$. Then, the PV output power of adjacent days is evaluated by cosine similarity [46] and correlation coefficient [47]. The metrics are defined as follows:

$$c_{ij} = \frac{\sum_{m=1}^{M} p_i^m p_j^m}{\sqrt{\sum_{m=1}^{M} (p_i^m)^2}\sqrt{\sum_{m=1}^{M} (p_j^m)^2}} \tag{2}$$

$$r_{ij} = \frac{\sum_{m=1}^{M} (p_i^m - p_i^{avg})(p_j^m - p_j^{avg})}{\sqrt{\sum_{m=1}^{M} (p_i^m - p_i^{avg})^2 (p_j^m - p_j^{avg})^2}} \tag{3}$$

$$C_k = \frac{1}{D-k} \sum_{i=1, j=i+k}^{D-k} c_{ij}, \quad R_k = \frac{1}{D-k} \sum_{i=1, j=i+k}^{D-k} r_{ij} \tag{4}$$

where $j \in [1, \ldots, D]$ and p_j^m is the mth output power point in the jth day, $p_j = [p_j^1, \ldots, p_j^M]^T$. k is an interval value between the ith day and the jth day, $i + k = j$. p_i^{avg} and p_j^{avg} are the average values of the ith day and jth day respectively. c_{ij} and r_{ij} are cosine similarity and correlation coefficient between the ith day and jth day, respectively. C_k is the average value of cosine similarity with the same k. Similarly, R_k is the average value of correlation coefficient.

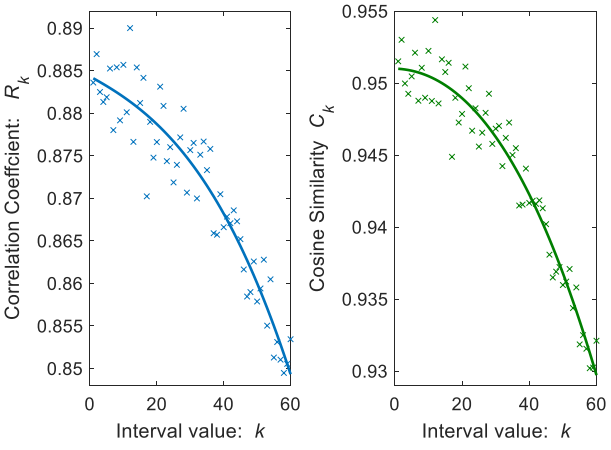

FIGURE 3. The average similarity degree.

In Fig. 3, we calculate the C_k and R_k with $k \in [1, \ldots, K]$, and $K = 60$. The results of the polynomial regression are also plotted in the figure. As shown in the plots, both the

metrics decrease with the increase of k. It can be inferred that the weather conditions may differ greatly when k is large. Especially when k is small, the adjacent days have a higher cosine similarity and correlation coefficient, that is, weather conditions may change little in these days. This implies that considering the PV data of the adjacent days can provide more information to forecast the future output power. Hence, the PV data of the adjacent days to improve prediction performance of PV systems is utilized.

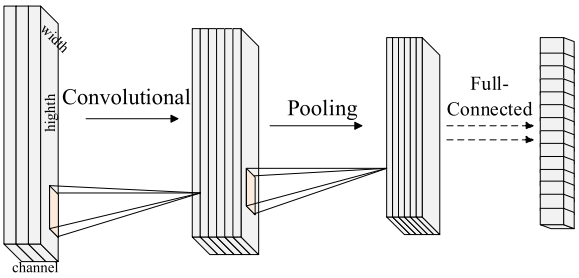

FIGURE 4. The structure of CNN.

III. THE FORECASTING ARCHITECTURE BASED ON CNN AND LSTM

A. CONVOLUTIONAL NEURAL NETWORK

CNN is a class of deep learning architecture that has been applied in various domains and achieved good performance [48], [49]. Generally, CNN is regarded as a hierarchical feature extractor, which can automatically learn high-level features from original sequences. The basic structure of CNN is shown in Fig. 4, including several types of layers, such as convolutional layer, pooling layer, and fully connected layer [50], [51]. The tasks of each layer are summarized as follows:

- **Convolution layer** is a fundamental component of CNN, which contains several convolution kernels to generate new feature maps. The convolution operation performs well in local feature extraction, where the kernel weights are shared across all input maps.
- **Pooling layer** is usually used to reduce the in-plane dimensionality of input maps, thereby decreasing the number of learnable parameters and helping to avoid overfitting. The pooling operations can be different types, such as max pooling, and average pooling.
- **Fully connected layer** is often used for high-level inference, which maps the features processed by the convolution layers and the pooling layers to the output layer.

In addition, the convolution layers (or pooling layer) is equipped with a nonlinear activation function, such as hyperbolic tangent function (tanh), and rectified linear unit (ReLU).

B. LONG-SHORT-TERM MEMORY NEURAL NETWORK

LSTM is an advanced architecture of recurrent neural networks (RNN) which can learn long-range dependencies [44], [52]. Fig. 5 shows the structure of an LSTM block,

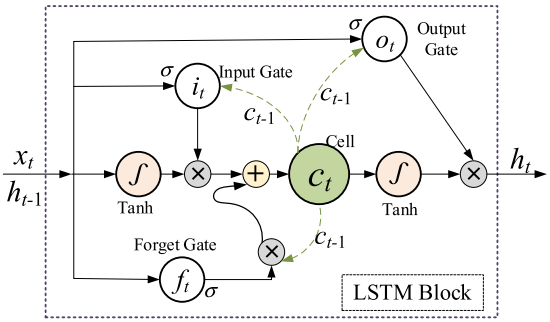

FIGURE 5. The structure of an LSTM block.

which contains an input gate i_t, a forget gate f_t, an output gate o_t, a memory cell c_t, and an outputs h_t. The current inputs x_t and the previous outputs h_{t-1} are the two external sources for the block. Input gate governs the inputs to update the memory cell, and forget gate sets what information to throw away from the block. The output gate controls what to output based on the inputs x_t, previous outputs h_{t-1} and memory cell c_t. The recursive computations of the LSTM block are as follow:

$$i_t = \sigma\left(W_{xi}x_t + W_{hi}h_{t-1} + W_{ci}c_{t-1} + b_i\right) \quad (5)$$

$$f_t = \sigma\left(W_{xf}x_t + W_{hf} + W_{cf}c_{t-1} + b_f\right) \quad (6)$$

$$c_t = f_t \odot c_{t-1} + i_t \odot \tanh\left(W_{xc}x_t + W_{hc}h_{t-1} + b_c\right) \quad (7)$$

$$o_t = \sigma\left(W_{xo}x_t + W_{ho}h_{t-1} + W_{co}c_t + b_o\right) \quad (8)$$

$$h_t = o_t \odot \tanh\left(c_t\right) \quad (9)$$

where $\odot$ denotes element-wise product, $\sigma(\cdot)$ is the sigmoid function, ie., $\sigma(x) = 1/(1+e^{-x})$. W_{xi} is the weight matrix between current inputs x_t and input gate i_t. b_i is the bias term. Similarly, the other weight matrixes in the forget gate, output gate, and memory cell have the same conditions. Unlike the traditional RNN, the memory cell c_t of LSTM will accumulate activities over time, ensuring the gradient can pass across multiple time steps.

C. IMPLEMENTATION OF THE HYBRID METHOD

To predict PV power accurately, we employ a hybrid approach based on CNN and LSTM to learn the specific input/output relationships automatically and adaptively. The architecture of the proposed method is shown in Fig. 6. We leverage a CNN model to forecast the output power p_d^{m+1} by the previous output power at $m+1$ in adjacent days. We believe that these PV power, such as p_{d-1}^{m+1} and p_{d-2}^{m+1}, can provide more information about the weather conditions, and also facilitate the prediction of p_d^{m+1}. From the output power matrix $\tilde{\boldsymbol{P}} \in \mathbf{R}^{D\times M}$, we can get a vector of the previous output power data, i.e.,

$$X_d = [p_{d-1}^{m+1}, p_{d-2}^{m+1} \ldots, p_{d-K}^{m+1}]^T \in \mathbf{R}^K \quad (10)$$

where p_{d-1}^{m+1} is the output power at the $(m+1)$th time on $(d\text{-}1)$th day. Next, $X_d \in \mathbf{R}^K$ is reshaped into an image $X_c \in \mathbf{R}^{H\times W}$ with height H and width W. Note that the

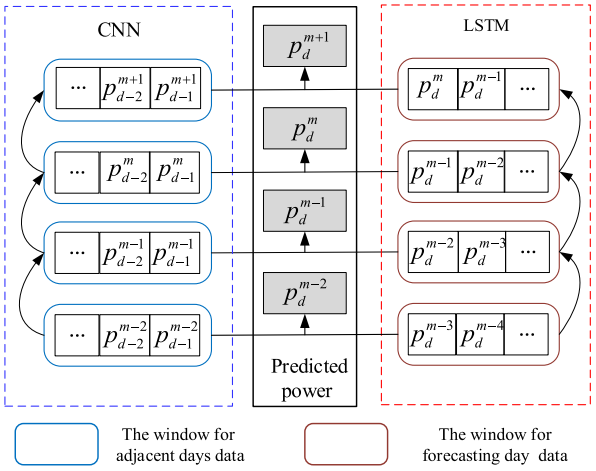

FIGURE 6. The architecture of the proposed method for PV power forecasting.

window size is immutable once the input size of the CNN is determined. As depicted in Fig. 6, LSTM predicts the next output power p_d^{m+1} by the latest output power, such as p_d^m. LSTM can model the temporal changes of the latest data to obtain good forecasting results. Similarly, the inputs of LSTM are as follows,

$$X_m=[p_d^m, p_d^{m-1} \ldots, p_d^{m-F}]^T \in \mathbf{R}^F \tag{11}$$

where p_d^m is the output power at the mth time on dth day. $X_m \in \mathbf{R}^F$ and F are the inputs and the window size of LSTM respectively.

Then, the prediction results of the proposed method take the CNN and LSTM models into consideration comprehensively. The true regression is estimated by fusing the estimates from CNN and LSTM, expressed as,

$$P^f = \alpha P^f_{\text{CNN}} + \beta P^f_{\text{LSTM}} \tag{12}$$

where P^f is the predicted output power of the proposed method. P^f_{CNN} and P^f_{LSTM} are the prediction results of CNN and LSTM respectively. Two non-negative weights α and β are assigned to the CNN and LSTM, respectively. Typically, the non-negative weight satisfies $\alpha + \beta = 1$, and it is a better idea to take the average of the prediction results. In addition, all parameters of CNN are jointly optimized through back propagation by minimizing the loss function defined on the dedicated task, and the parameters of LSTM are optimized by back propagation through time (BPTT).

D. PERFORMANCE EVALUATION SCHEME

Usually, the prediction performance of the models is evaluated by comparing the difference between the predicted value and the measured value. The precision of the estimation of PV output power can be investigated by mean absolute error (MAE) and root mean square error (RMSE) [4], and coefficient of determination (R^2) [53]. The evaluation criteria are as follows:

$$\text{MAE} = \frac{1}{N}\sum_{n\in N}\left|P_n^m - P_n^f\right| \tag{13}$$

$$\text{RMSE} = \sqrt{\frac{1}{N}\sum_{n\in N}\left(P_n^m - P_n^f\right)^2} \tag{14}$$

$$\text{R}^2 = 1 - \frac{\sum_{n\in N}\left(P_n^m - P_n^f\right)^2}{\sum_{n\in N}\left(P_n^m - P_{avg}^m\right)^2}, \quad P_{avg}^m = \frac{1}{N}\sum_{n\in N} P_n^m \tag{15}$$

where N is the total number of test samples, P_n^m and P_n^f are the measured and predicted output power, respectively. P_{avg}^m is the average of the measured power in the test set. It is worth noting that the predictive model has higher accuracy when MAE and RMSE are smaller, and the predictive model is more efficient when R^2 closer to 1.

IV. NUMERICAL RESULTS AND ANALYSIS

A. THE DESCRIPTION OF DATASET

In the simulation, the historical PV output power data were collected by Elia, the Belgium's electricity transmission system operator, which can be downloaded for free and found in the literature [54]. The prediction model is trained and tested by using the dataset of Limberg PV power plant. Note that the active power flow meter is used to measure the active power of the PV plants in real time, and the measurement error of the power flow meter is within 0.5%. Since the measurement error is usually small, the measured power used in this article is regarded as the actual output power of the PV plants. Hence, just like other PV power prediction articles, the measurement errors are not considered in the experiments.

For the data sets, the rated capacity of the PV power plant is 451.82 MW, and the minimum output power is 0 MW. The dataset covers the period from March 2015 to March 2016, with a resolution of 15 minutes. To evaluate the generalization capabilities of these forecasting methods comprehensively, the forecasting horizons range from 15-min ahead to 180-min ahead is considered. The data set is divided into four cases by season, namely spring, summer, fall and winter. For each season, the data set is divided two subsets: the training set and testing set are used to train prediction models and evaluate the forecasting performance of prediction models, respectively. Herein, each season contains three months of data, wherein the first two months of data are used for training, and remaining data is used for testing. In addition, three benchmark methods based on Persistence [55], BPNN [41], and RBFNN [42] are selected to compare with the proposed method. Note that the prediction model is trained and tested independently in each season.

B. 15-MIN AHEAD FORECAST RESULTS

In each of the four seasons, the MAE and RMSE metrics of 15-min ahead are shown in Table 1. From Table 1, the metrics fluctuate obviously in different seasons, the MAE of the

TABLE 1. Performance evaluation for the 15-min ahead forecast.

Season	Error	Persistence	BPNN	RBFNN	Proposed
Spring	MAE	6.111	2.777	2.716	1.654
	RMSE	9.354	5.424	5.185	3.206
Summer	MAE	5.429	1.690	1.606	0.997
	RMSE	8.443	2.787	2.746	1.664
Fall	MAE	2.181	0.963	0.995	0.584
	RMSE	4.674	2.432	2.375	1.448
Winter	MAE	2.816	2.090	1.246	0.876
	RMSE	5.945	5.997	2.863	2.062
Average	MAE	4.134	1.880	1.641	1.028
	RMSE	7.104	4.160	3.292	2.095

proposed method ranges from a low of 0.0.876 to a high of 1.654, with an average of 1.028. While the average MAE of Persistence, BPNN, RBFNN are 4.134, 1.880, and 1.641, respectively. For the RMSE metric, the average values of Persistence, BPNN, RBFNN and the proposed method are 7.104, 4.160, 3.292, and 2.095, respectively. Compared with the Persistence, BPNN, RBFNN methods, the MAE metric has been averagely decreased by 3.016, 0.852, and 0.613, respectively, and RMSE by 5.009, 2.065, and 1.197, respectively. It turns out that the proposed method outperforms three benchmark methods and has good performance in the prediction horizon of 15-min ahead.

TABLE 2. Performance evaluation for the 45-min ahead forecast.

Season	Error	Persistence	BPNN	RBFNN	Proposed
Spring	MAE	17.646	8.980	8.953	5.383
	RMSE	26.499	16.062	15.701	9.565
Summer	MAE	16.047	6.274	5.574	3.624
	RMSE	24.698	9.894	9.608	5.879
Fall	MAE	6.329	3.551	3.626	2.146
	RMSE	13.264	7.249	7.281	4.356
Winter	MAE	8.251	5.105	3.959	2.781
	RMSE	17.144	11.672	8.400	5.815
Average	MAE	12.068	5.978	5.528	3.484
	RMSE	20.401	11.219	10.248	6.404

C. 45-MIN AHEAD FORECAST RESULTS

For the 45-min ahead forecast, we show the MAE and RMSE metrics of these forecasting methods in Table 2. Obviously, the error of these methods increase as the prediction horizon increases. Table 2 shows that for the Persistence, BPNN, RBFNN and the proposed method, the average MAE metrics are 12.068, 5.978, 5.528, and 3.484, respectively. Similarly, the average RMSE metrics by 20.401, 11.219, 10.248, and 6.404, respectively. From the average metrics, the Persistence model is the worst and has large prediction errors, which may be caused by its prediction mechanism. The Persistence model is not suitable for multi-step prediction because it assumes that the output power at $t+1$ is equal to the output power at t. As for BPNN and RBFNN, they provide better prediction performance than Persistence method for 45-min ahead prediction horizon. However, these shallow forecasting models cannot effectively extract the non-linearity and complexity features exhibited in the PV data. Compared with the Persistence, BPNN, RBFNN methods, the MAE metric of the proposed method has been averagely decreased by 8.584, 2.494, and 2.004, respectively, and RMSE by 13.997, 4.185, and 3.844, respectively. These results reveal the effectiveness of the proposed method further.

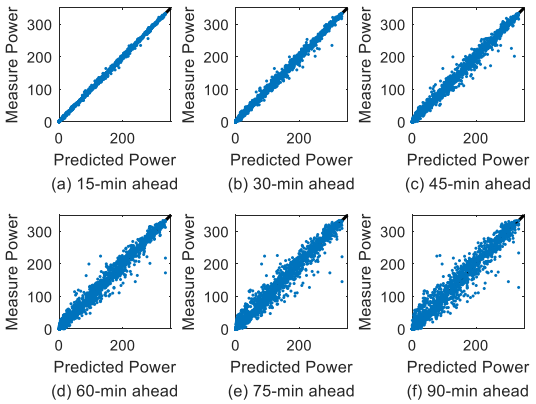

FIGURE 7. The Scatter plot of predicted power and measured power in summer.

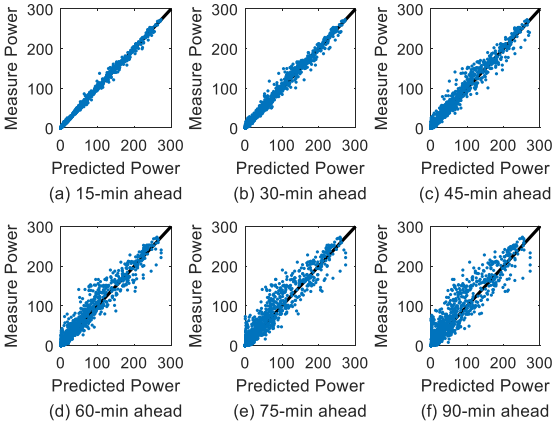

FIGURE 8. The Scatter plot of predicted power and measured power in winter.

D. SCATTER PLOT OF FORECAST RESULTS

Then, the scatter plots of the proposed method in Summer and Winter are shown in Fig. 7 and Fig. 8. The prediction horizons range from 15-min ahead to 90-min ahead, and the baselines are black in the plots. We remark that the horizontal axis of these subgraphs is the predicted power and the vertical axis is the measured power. For 15-min ahead forecast, the scatter plot converges well to the baseline, which demonstrates that the predicted results match with the measured results exactly. For 45-min ahead forecast, some blue points deviate significantly from the baseline. From the Fig. 7 and Fig. 8, it is obvious that the deviation between the predicted power and

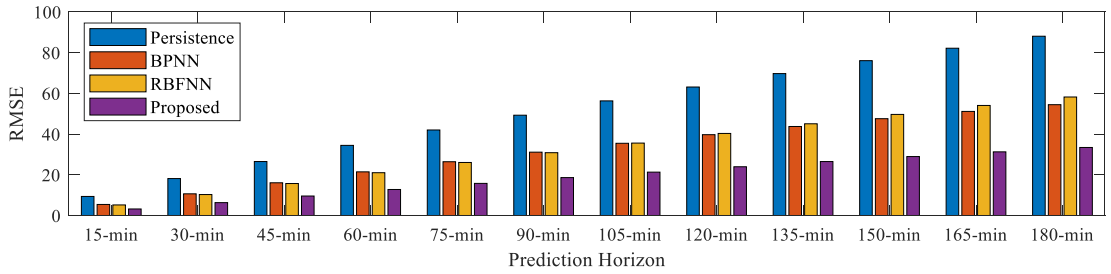

FIGURE 9. The RMSE statistics for various forecasting horizons in spring.

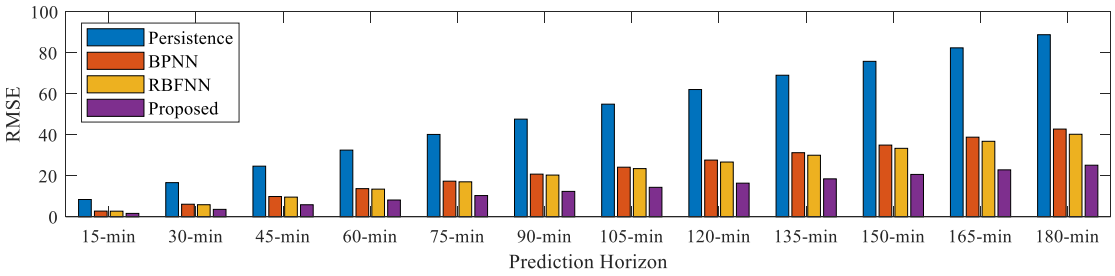

FIGURE 10. The RMSE statistics for various forecasting horizons in summer.

the measured power increases with the increase of the prediction horizon. In addition, the performance of the proposed method is better in summer than that in winter because of the solar irradiance of Limberg in summer is stronger than in winter.

TABLE 3. The coefficient of determination R^2.

Season	15-min	30-min	45-min	60-min	75-min	90-min
Spring	0.9984	0.9912	0.9854	0.9650	0.9392	0.9180
Summer	0.9993	0.9968	0.9916	0.9838	0.9746	0.9642
Fall	0.9966	0.9869	0.9768	0.9579	0.9299	0.9070
Winter	0.9974	0.9906	0.9767	0.9556	0.9289	0.9057

In practice, accurate prediction of PV power helps to reduce the uncertainty and volatility in the estimation of PV power. To verify the competitiveness of the proposed method further, R^2 is used to measure the goodness-of-fit in the four seasons. Note that the predictive model will be more effective when R^2 closer to 1. Table 3 shows the R^2 for the four seasons, with the prediction horizon ranges from 15-min ahead to 90-min ahead. In the table, the proposed method exhibits the values of R^2 (0.9180∼0.9984) in spring, R^2 (0.9642∼0.9993) in summer, R^2 (0.9070∼0.9966) in fall, and R^2 (0.9057∼0.9974) in winter. The R^2 metric obtained from these seasons varies from a low of 0.9057 to a high of 0.9993. These results indicate that the proposed method has a higher forecast capability in term of various prediction horizons. Meanwhile, R^2 will be affected by the local season in Limberg, as the solar irradiance and temperature vary significantly from season to season. The R^2 of summer and winter can be proved in Fig. 7 and Fig. 8.

E. MUTI-STEP AHEAD FORECAST FOR LIMBERG

Furthermore, Fig. 9, Fig. 10, Fig. 11, and Fig. 12 show the RMSE for spring, summer, fall, and winter, respectively. In each season, the forecasting horizons range from 15-min ahead to 180-min ahead, and the Persistence, BPNN, RBFNN are plotted as benchmarks. Obviously, the RMSE of these methods increases linearly with the increase of prediction horizon. The results at each prediction horizon generated by Persistence method are the worst compared to other benchmarks. It can be seen that the proposed method can provide good forecasting performance in the four seasons. Moreover, at all prediction horizons in the case studies, the proposed method has the smallest RMSE metrics, which shows the best forecasting performance compared to other methods. Statistically, the RMSE obtained from the proposed method ranges from 3.206 to 33.405 in spring, from 1.664 to 25.166 in summer, from 1.448 to 19.806 in fall, and from 2.062 to 21.223 in winter. Compared with averagely RMSE metrics from BPNN and RBFNN methods, the improvement grows from 2.065 to 17.766, and from 1.197 to 1.867, respectively. The RMSE of the proposed method has a minimum value of 1.448 and a maximum value of 33.405 in all seasons, which is much better than BPNN and RBFNN. Furthermore, Table 4 shows the average MAE metric for Persistence, BPNN, RBFNN, and the proposed method in different prediction horizons. The results in Table 4 also show that the proposed method outperforms the other methods in all the time horizons.

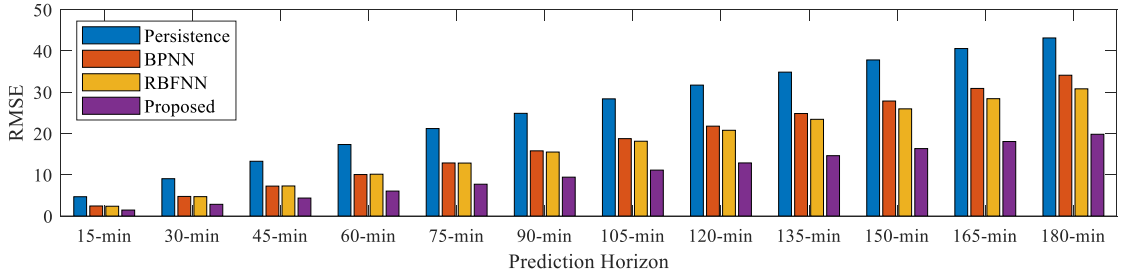

FIGURE 11. The RMSE statistics for various forecasting horizons in fall.

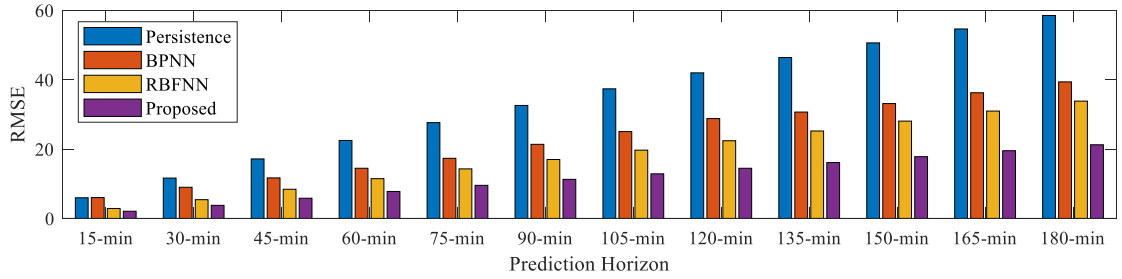

FIGURE 12. The RMSE statistics for various forecasting horizons in winter.

TABLE 4. Average MAE statistics in terms of various prediction horizons.

Method	15-min	30-min	45-min	60-min	75-min	90-min	105-min	120-min	135-min	150-min	165-min	180-min
Persistence	4.143	8.162	12.081	15.915	19.637	23.270	26.839	30.343	33.780	37.147	40.424	43.618
BPNN	1.880	3.829	5.978	8.259	10.583	13.029	15.484	18.042	20.548	23.177	25.994	28.903
RBFNN	1.641	3.434	5.528	7.812	10.119	12.420	14.744	17.126	19.566	22.026	24.523	26.992
Proposed	1.028	2.167	3.484	4.898	6.321	7.753	9.199	10.699	12.256	13.865	15.536	17.236

V. CONCLUSION

This article addresses the short-term prediction problem in PV power generation systems through the artificial intelligent technology. We establish a hybrid deep learning framework and associate the previous data of adjacent days that can prove to be extremely useful in practice. Unlike the traditional short-term prediction methods, CNN is employed to extract key weather change features of PV power from the sequences at the same time on different dates. LSTM also efficiently provide reliable estimates of the next time by the previous PV power data on the same date due to their recurrent architecture and memory units. The proposed hybrid method is compared with three benchmark methods based on Persistence, BPNN, and RBFNN. The solar power dataset used for these forecasting methods is collected from actual wind plants in Limberg. Relevant simulation results demonstrate that the proposed method provides very small prediction errors compared with the benchmark methods. In addition, we would like to point out that while the focus of this work is on the short-term prediction problem of PV power generation, the proposed method can be used to promote the future application of solar energy in electrical power and energy systems.

REFERENCES

[1] I.-Y. Joo and D.-H. Choi, "Distributed optimization framework for energy management of multiple smart homes with distributed energy resources," *IEEE Access*, vol. 5, pp. 15551–15560, 2017.

[2] D. Xu, Q. Wu, B. Zhou, C. Li, L. Bai, and S. Huang, "Distributed multi-energy operation of coupled electricity, heating, and natural gas networks," *IEEE Trans. Sustain. Energy*, vol. 11, no. 4, pp. 2457–2469, Oct. 2020.

[3] B. Kumar Sahu, "A study on global solar PV energy developments and policies with special focus on the top ten solar PV power producing countries," *Renew. Sustain. Energy Rev.*, vol. 43, pp. 621–634, Mar. 2015.

[4] H. Wang, H. Yi, J. Peng, G. Wang, Y. Liu, H. Jiang, and W. Liu, "Deterministic and probabilistic forecasting of photovoltaic power based on deep convolutional neural network," *Energy Convers. Manage.*, vol. 153, pp. 409–422, Dec. 2017.

[5] Li, Wang, Zhang, Xin, and Liu, "Recurrent neural networks based photovoltaic power forecasting approach," *Energies*, vol. 12, no. 13, p. 2538, Jul. 2019.

[6] J. Antonanzas, N. Osorio, R. Escobar, R. Urraca, F. J. Martinez-de-Pison, and F. Antonanzas-Torres, "Review of photovoltaic power forecasting," *Sol. Energy*, vol. 136, pp. 78–111, Oct. 2016.

[7] H. Wang, Z. Lei, X. Zhang, B. Zhou, and J. Peng, "A review of deep learning for renewable energy forecasting," *Energy Convers. Manage.*, vol. 198, Oct. 2019, Art. no. 111799.

[8] Y. Riffonneau, S. Bacha, F. Barruel, and S. Ploix, "Optimal power flow management for grid connected PV systems with batteries," *IEEE Trans. Sustain. Energy*, vol. 2, no. 3, pp. 309–320, Jul. 2011.

[9] G. B. M. A. Litjens, E. Worrell, and W. G. J. H. M. van Sark, "Assessment of forecasting methods on performance of photovoltaic-battery systems," *Appl. Energy*, vol. 221, pp. 358–373, Jul. 2018.

[10] C. Chen, S. Duan, B. Liu, and G. Hu, "Smart energy management system for optimal microgrid economic operation," *IET Renew. Power Generat.*, vol. 5, no. 3, pp. 258–267, 2011.

[11] W. Ma, W. Wang, X. Wu, R. Hu, F. Tang, W. Zhang, X. Han, and L. Ding, "Optimal allocation of hybrid energy storage systems for smoothing photovoltaic power fluctuations considering the active power curtailment of photovoltaic," *IEEE Access*, vol. 7, pp. 74787–74799, 2019.

[12] H. Ming, B. Xia, K.-Y. Lee, A. Adepoju, S. Shakkottai, and L. Xie, "Prediction and assessment of demand response potential with coupon incentives in highly renewable power systems," *Protection Control Modern Power Syst.*, vol. 5, no. 1, pp. 1–14, Dec. 2020.

[13] S. K. Injeti and V. K. Thunuguntla, "Optimal integration of DGs into radial distribution network in the presence of plug-in electric vehicles to minimize daily active power losses and to improve the voltage profile of the system using bio-inspired optimization algorithms," *Protection Control Modern Power Syst.*, vol. 5, no. 1, pp. 1–15, Dec. 2020.

[14] W. Jiang and Y. Zhen, "A real-time EV charging scheduling for parking lots with PV system and energy store system," *IEEE Access*, vol. 7, pp. 86184–86193, 2019.

[15] H. Kikusato, K. Mori, S. Yoshizawa, Y. Fujimoto, H. Asano, Y. Hayashi, A. Kawashima, S. Inagaki, and T. Suzuki, "Electric vehicle Charge–Discharge management for utilization of photovoltaic by coordination between home and grid energy management systems," *IEEE Trans. Smart Grid*, vol. 10, no. 3, pp. 3186–3197, May 2019.

[16] M. B. Shadmand and R. S. Balog, "Multi-objective optimization and design of photovoltaic-wind hybrid system for community smart DC microgrid," *IEEE Trans. Smart Grid*, vol. 5, no. 5, pp. 2635–2643, Sep. 2014.

[17] D. Q. Hung, N. Mithulananthan, and K. Y. Lee, "Determining PV penetration for distribution systems with time-varying load models," *IEEE Trans. Power Syst.*, vol. 29, no. 6, pp. 3048–3057, Nov. 2014.

[18] G. Wang, X. Zhang, H. Wang, J.-C. Peng, H. Jiang, Y. Liu, C. Wu, Z. Xu, and W. Liu, "Robust planning of electric vehicle charging facilities with an advanced evaluation method," *IEEE Trans. Ind. Informat.*, vol. 14, no. 3, pp. 866–876, Mar. 2018.

[19] X. Wu, X. Hu, S. Moura, X. Yin, and V. Pickert, "Stochastic control of smart home energy management with plug-in electric vehicle battery energy storage and photovoltaic array," *J. Power Sources*, vol. 333, pp. 203–212, Nov. 2016.

[20] K. Wang, X. Qi, and H. Liu, "A comparison of day-ahead photovoltaic power forecasting models based on deep learning neural network," *Appl. Energy*, vol. 251, Oct. 2019, Art. no. 113315.

[21] G. E. Box, G. M. Jenkins, G. C. Reinsel, and G. M. Ljung, *Time Series Analysis: Forecasting and Control*. Hoboken, NJ, USA: Wiley, 2015.

[22] Y. Li, Y. He, Y. Su, and L. Shu, "Forecasting the daily power output of a grid-connected photovoltaic system based on multivariate adaptive regression splines," *Appl. Energy*, vol. 180, pp. 392–401, Oct. 2016.

[23] Y.-Z. Li, R. Luan, and J.-C. Niu, "Forecast of power generation for grid-connected photovoltaic system based on grey model and Markov chain," in *Proc. 3rd IEEE Conf. Ind. Electron. Appl.*, Jun. 2008, pp. 1729–1733.

[24] R. H. Inman, H. T. C. Pedro, and C. F. M. Coimbra, "Solar forecasting methods for renewable energy integration," *Prog. Energy Combustion Sci.*, vol. 39, no. 6, pp. 535–576, Dec. 2013.

[25] J. Alonso-Montesinos and F. J. Batlles, "Solar radiation forecasting in the short- and medium-term under all sky conditions," *Energy*, vol. 83, pp. 387–393, Apr. 2015.

[26] R. Perez, S. Kivalov, J. Schlemmer, K. Hemker, D. Renné, and T. E. Hoff, "Validation of short and medium term operational solar radiation forecasts in the US," *Sol. Energy*, vol. 84, no. 12, pp. 2161–2172, Dec. 2010.

[27] H.-Z. Wang, G.-Q. Li, G.-B. Wang, J.-C. Peng, H. Jiang, and Y.-T. Liu, "Deep learning based ensemble approach for probabilistic wind power forecasting," *Appl. Energy*, vol. 188, pp. 56–70, Feb. 2017.

[28] H. Wang, Y. Liu, B. Zhou, C. Li, G. Cao, N. Voropai, and E. Barakhtenko, "Taxonomy research of artificial intelligence for deterministic solar power forecasting," *Energy Convers. Manage.*, vol. 214, Jun. 2020, Art. no. 112909.

[29] X. Yuan, L. Li, Y. Shardt, Y. Wang, and C. Yang, "Deep learning with spatiotemporal attention-based LSTM for industrial soft sensor model development," *IEEE Trans. Ind. Electron.*, early access, Apr. 13, 2020, doi: 10.1109/TIE.2020.2984443.

[30] G. Li, S. X. Wu, S. Zhang, and Q. Li, "Neural networks-aided insider attack detection for the average consensus algorithm," *IEEE Access*, vol. 8, pp. 51871–51883, 2020.

[31] D. Xu, J. Liu, X.-G. Yan, and W. Yan, "A novel adaptive neural network constrained control for a multi-area interconnected power system with hybrid energy storage," *IEEE Trans. Ind. Electron.*, vol. 65, no. 8, pp. 6625–6634, Aug. 2018.

[32] X. Yuan, J. Zhou, B. Huang, Y. Wang, C. Yang, and W. Gui, "Hierarchical quality-relevant feature representation for soft sensor modeling: A novel deep learning strategy," *IEEE Trans. Ind. Informat.*, vol. 16, no. 6, pp. 3721–3730, Jun. 2020.

[33] W. Qiao, K. Huang, M. Azimi, and S. Han, "A novel hybrid prediction model for hourly gas consumption in supply side based on improved whale optimization algorithm and relevance vector machine," *IEEE Access*, vol. 7, pp. 88218–88230, 2019.

[34] A. Ullah, J. Ahmad, K. Muhammad, M. Sajjad, and S. W. Baik, "Action recognition in video sequences using deep bi-directional LSTM with CNN features," *IEEE Access*, vol. 6, pp. 1155–1166, 2018.

[35] W. Liu, M. Zhang, Z. Luo, and Y. Cai, "An ensemble deep learning method for vehicle type classification on visual traffic surveillance sensors," *IEEE Access*, vol. 5, pp. 24417–24425, 2017.

[36] X. Yuan, C. Ou, Y. Wang, C. Yang, and W. Gui, "A layer-wise data augmentation strategy for deep learning networks and its soft sensor application in an industrial hydrocracking process," *IEEE Trans. Neural Netw. Learn. Syst.*, early access, Dec. 13, 2020, doi: 10.1109/TNNLS.2019.2951708.

[37] T. Yang, B. Li, and Q. Xun, "LSTM-Attention-Embedding model-based day-ahead prediction of photovoltaic power output using Bayesian optimization," *IEEE Access*, vol. 7, pp. 171471–171484, 2019.

[38] D. Gotleyb, G. L. Sciuto, C. Napoli, R. Shikler, E. Tramontana, and M. Wozniak, "Characterisation and modeling of organic solar cells by using radial basis neural networks," in *Proc. ICAISC (1)*, in Lecture Notes in Computer Science, vol. 9692. Springer, 2016, pp. 91–103.

[39] H. Z. Wang, G. B. Wang, G. Q. Li, J. C. Peng, and Y. T. Liu, "Deep belief network based deterministic and probabilistic wind speed forecasting approach," *Appl. Energy*, vol. 182, pp. 80–93, Nov. 2016.

[40] C.-J. Huang and P.-H. Kuo, "Multiple-input deep convolutional neural network model for short-term photovoltaic power forecasting," *IEEE Access*, vol. 7, pp. 74822–74834, 2019.

[41] J. Liu, W. Fang, X. Zhang, and C. Yang, "An improved photovoltaic power forecasting model with the assistance of aerosol index data," *IEEE Trans. Sustain. Energy*, vol. 6, no. 2, pp. 434–442, Apr. 2015.

[42] C. Chen, S. Duan, T. Cai, and B. Liu, "Online 24-h solar power forecasting based on weather type classification using artificial neural network," *Sol. Energy*, vol. 85, no. 11, pp. 2856–2870, Nov. 2011.

[43] A. Mellit, A. Massi Pavan, and V. Lughi, "Short-term forecasting of power production in a large-scale photovoltaic plant," *Sol. Energy*, vol. 105, pp. 401–413, Jul. 2014.

[44] M. Abdel-Nasser and K. Mahmoud, "Accurate photovoltaic power forecasting models using deep LSTM-RNN," *Neural Comput. Appl.*, vol. 31, pp. 2727–2740, Jul. 2019.

[45] W. Lee, K. Kim, J. Park, J. Kim, and Y. Kim, "Forecasting solar power using long-short term memory and convolutional neural networks," *IEEE Access*, vol. 6, pp. 73068–73080, 2018.

[46] Y.-J. He, Y.-C. Zhu, J.-C. Gu, and C.-Q. Yin, "Similar day selecting based neural network model and its application in short-term load forecasting," in *Proc. Int. Conf. Mach. Learn. Cybern.*, vol. 8, 2005, pp. 4760–4763.

[47] X. Sun, P. B. Luh, K. W. Cheung, W. Guan, L. D. Michel, S. S. Venkata, and M. T. Miller, "An efficient approach to short-term load forecasting at the distribution level," *IEEE Trans. Power Syst.*, vol. 31, no. 4, pp. 2526–2537, Jul. 2016.

[48] A. Krizhevsky, I. Sutskever, and G. E. Hinton, "Imagenet classification with deep convolutional neural networks," in *Proc. Adv. Neural Inf. Process. Syst. (NIPS)*, 2012, pp. 1097–1105.

[49] Z. J. Wang, R. Turko, O. Shaikh, H. Park, N. Das, F. Hohman, M. Kahng, and D. H. Chau, "CNN explainer: Learning convolutional neural networks with interactive visualization," 2020, *arXiv:2004.15004*. [Online]. Available: http://arxiv.org/abs/2004.15004

[50] G. Li, S. X. Wu, S. Zhang, and Q. Li, "Detect insider attacks using CNN in decentralized optimization," in *Proc. IEEE Int. Conf. Acoust., Speech Signal Process. (ICASSP)*, May 2020, pp. 8758–8762.

[51] R. Yamashita, M. Nishio, R. K. G. Do, and K. Togashi, "Convolutional neural networks: An overview and application in radiology," *Insights into Imag.*, vol. 9, no. 4, pp. 611–629, Aug. 2018.

[52] W. Zhu, C. Lan, J. Xing, W. Zeng, Y. Li, L. Shen, and X. Xie, "Co-occurrence feature learning for skeleton based action recognition using regularized deep LSTM networks," in *Proc. AAAI*. New Orleans, LA, USA: AAAI Press, 2016, pp. 3697–3704.
[53] A. S. B. Mohd Shah, H. Yokoyama, and N. Kakimoto, "High-precision forecasting model of solar irradiance based on grid point value data analysis for an efficient photovoltaic system," *IEEE Trans. Sustain. Energy*, vol. 6, no. 2, pp. 474–481, Apr. 2015.
[54] Elia. *Belgium's Electricity Transmission System Operator*. Accessed: Jan. 13, 2020. [Online]. Available: https://www.elia.be/en/grid-data/power-generation/solar-pv-power-generation-data
[55] C. Yang, A. A. Thatte, and L. Xie, "Multitime-scale data-driven spatio-temporal forecast of photovoltaic generation," *IEEE Trans. Sustain. Energy*, vol. 6, no. 1, pp. 104–112, Jan. 2015.

GANGQIANG LI received the B.Eng. degree in electronic engineering from the Henan University of Urban Construction, Pingdingshan, China, in 2014, and the M.Eng. degree in control science and engineering from Shenzhen University, Shenzhen, China, in 2017, where he is currently pursuing the Ph.D. degree with the College of Electronics and Information Engineering. His research interests include machine learning and power system planning and operation.

SEN XIE received the B.Eng. degree in electrical engineering and automation from the Hunan University of Technology, China, in 2011, the M.Eng. degree in control theory and control engineering from Liaoning Technical University, China, in 2014, and the Ph.D. degree in control science and engineering from Central South University, China, in 2018. She is currently a Postdoctoral Researcher with Shenzhen University, China. Her research interests include modeling and optimal control of complex industrial process, data processing, and intelligent analysis.

BOZHONG WANG received the B.S. and M.S. degrees in electrical engineering from North China Electric Power University, Beijing, China, in 2009 and 2012, respectively. He is currently a Power Grid Engineer at Maintenance Company of State Grid Hunan Electric Power Corporation, Changsha, China. His major research interests include power system operation, reliability, maintenance, and protection.

JIANTAO XIN received the B.Eng. degree from the College of Electrical and Information Engineering, Hunan University of Technology, Shenzhen, China, in 2009, and the M.Eng. degree from the College of Engineering, South China Agricultural University, Shenzhen, China, in 2012. He is currently pursuing the Ph.D. degree with the College of Electronics and Information Engineering, Shenzhen University, Shenzhen. His research interests include machine learning, machine intelligence, communication systems, and economic dispatch.

YUNFENG LI received the B.Eng. degree in electrical engineering and the M.Eng. degree in signal detection from Jiangxi Normal University, in 2016 and 2019, respectively. He is currently pursuing the Ph.D. degree in communication and information engineering. His research interests include the Internet-of-Things technology, artificial intelligence, image processing, wearable smart devices, and blockchain.

SHENGNAN DU received the B.S. degree in electrical engineering and automation from the Henan University of Science and Technology, Luoyang, China, in 2019. She is currently pursuing the M.S. degree with the College of Electrical and Information Engineering, Hunan University, Changsha, Hunan, China. Her major research interest includes power system planning and operation.